1 Sampling and characterization of the Flaminio Stadium

1.1 Information on the monument

The Flaminio Stadium (Fig. 9.1), designed by Pier Luigi and Antonio Nervi, was built between 1957 and 1958 and inaugurated in 1959 on the occasion of the 17th Rome Olympics (1960). The stadium can contain about 50,000 spectators and also includes four gyms and a swimming pool located under the main stand, a bar, locker rooms and a first aid area. All the facilities were built with state-of-the-art building systems, using exposed reinforced concrete with a roof made of a partially prefabricated canopy. The maximum dimensions of the stadium were 181 m in length and 131 m in width, the total covered area was about 21 600 m^2 and the grass pitch measured 105x70 m. The load-bearing structure of the Flaminio stadium consists of a series of pillars (framework) arranged at a regular distance around the entire perimeter of the complex. On top of this structure the other elements, such as the terraces, were added. Nervi used reinforced concrete in a variety of ways, some of them unconventional, for example the in situ concrete castings for the large structural frameworks, the prefabricated elements for the terraces and in corrugated ferro-cement in specially-designed moulds. This latter application was used to produce the structure of the canopy, which is supported by inclined pillars leaned against the stadium's external structure. This monument is a unique construction that skilfully combines form and structure. It marries architecture and engineering in a most original way and testifies to a golden age in modern Italian architecture.

Pier Luigi Nervi was born in Sondrio, Italy, on 21st June 1891 and died in Rome on 9th January, 1979. He was an engineer and one of the most important architects of structural architecture on the international scene. He was a pioneer in the study and application of reinforced concrete, enjoying the great freedom in composition. Always attentive to the relationship between structure and form, he based his work on the concept of 'resistance by form', designing every part of his structures according to the internal forces they would be subjected to. Additionally, economic considerations in his projects frequently resulted in opportunities to adopt innovative techniques and to make good use of his highly-skilled workforce, even when rudimentary materials were used.

Figure 9.1. View of Flaminio Stadium

1.2 Sampling activities

The samples were taken according to non-invasive criteria from the monument in areas considered to be of interest due to the different properties of the materials and the state of conservation.

The samples (see figure 9.2) were selected considering the surfaces characteristics and differences in composition which emerged from visual observation. Particular attention was devoted to those areas highly degraded and exposed to the effects of weathering.

Given the size of Flaminio Stadium, several sampling areas were selected from different locations in the North, South, East and West sections (Table 9.1).

Table 9.1. List of the collected samples

Flaminio Stadium	- SF 1 – frame 92, sample of ferro-cement collected from the canopy - SF 2 – frame 1, sample of concrete collected from a connection point between a pillar frame and prefabricated element - SF 3 – sample of concrete collected from a prefabricated element of the grandstand - SF 4 – frame 73, sample of direct concrete cast collected from the pillar corner - SF 5 – frame 75, sample of direct concrete cast collected from the pillar wall - SF 6 – frame 29, sample of direct concrete cast collected from the stairs wall - SF 7 – frame 27, sample of direct concrete cast collected from the stairs wall - SF 8 – frame 8, sample of direct concrete cast collected from the external wall of the ground floor - SF 9 – frame 8, sample of direct concrete cast collected from the internal wall of the ground floor - SF 10b – frame 8, sample of direct concrete cast collected from the external wall of the first floor

This project has received funding from the European Union's Horizon 2020 Research and Innovation Programme under Grant Agreement Nº 760858

Sample SF1 – SF2: the sampling area of the canopy in ferro-cement showed concrete detachments, corroded rebar and presence of moisture caused by water infiltration.

Sample SF3: the area below the grandstand suffered from salts efflorescence and corroded rebar with detachments of cement material.

Sample SF4: the sampling area did not seem to be affected from degradation processes. The samples was collected in order to compare data from a previous characterisation of the pillar performed during an earlier measurements campaign.

Sample SF5: The pillar was subject to water infiltration from the above structure and exhibit corroded rebar with partial detachment of the concrete.

Sample SF6: Area selected from a surface exposed to weathering.

Sample SF7: The sampling area is located on the south part of the stadium and it appeared to be affected by erosion and concrete detachment.

Sample SF8 –SF9: the area presented internal problems of humidity and external problems of water infiltration.

Sample SF10b: the area showed water infiltration from the above structure and contact stress of adjacent metal barrier.



This project has received funding from the European Union's Horizon 2020 Research and Innovation Programme under Grant Agreement Nº 760858

This project has received funding from the European Union's Horizon 2020 Research and Innovation Programme under Grant Agreement Nº 760858

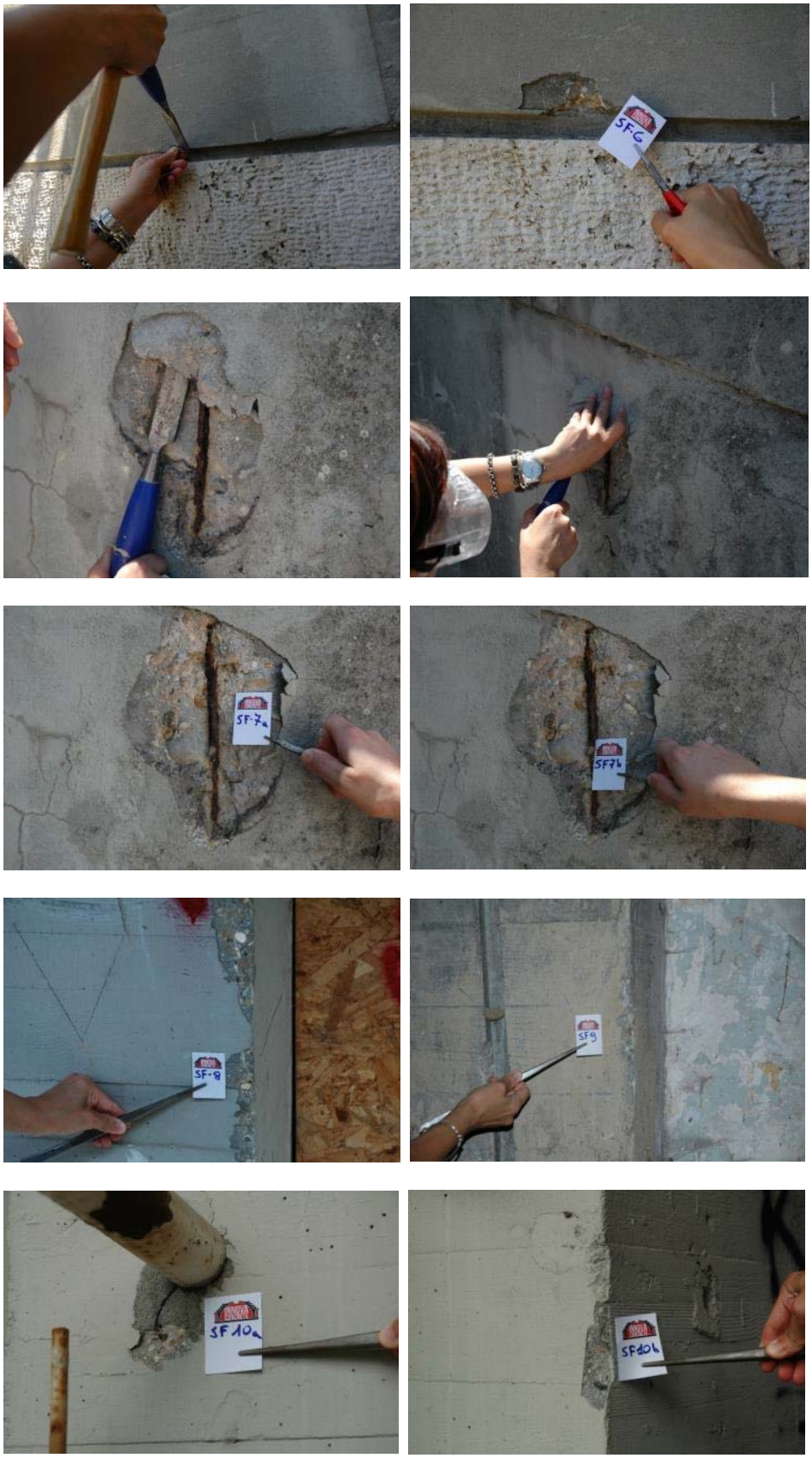

Figure 9.2. The photos show the samples collected and their position.

This project has received funding from the European Union's Horizon 2020 Research and Innovation Programme under Grant Agreement Nº 760858

1.3 Results of the characterization

The Flaminio Stadium selected as an additional case study was characterized to achieve information about its composition and state of conservation. In particular, the characterizations of the samples extracted from the monuments and in situ measurements were carried out by using complementary techniques. Details on the results of the characterizations are reported hereafter.

The most representative data are reported hereafter by talking into account the different use of concrete. The attention has been focused mainly on the pillars and large structural frames prepared by in situ casting and on the undulating slabs of ferrocement realised on site for the canopies.

Petrographic study of thin sections

The samples from the Flaminio Stadium are characterized by some differences in terms of composition and morphology. The main characteristics observed under optical microscope with transmitted light are reported in the table below.

First of all, the samples collected are characterized by a great heterogeneity in terms of percentage of aggregate, binder/aggregate ratio, and porosity (Fig. 9.3). The only common characteristic is the type of the matrix that is a mixed binder composed by air lime and cement. In only one case (SF3) out of six, the two components are well blended. In the other samples, the two binders are not homogenized, this is showed by the alternation of calcite-rich and calcite-poor parts. The cementitious fraction seems to prevail on the air lime one. The opaque particles dark in colour, residues of fired clinker, are uniformly distributed in all the sample. Their dimensions vary from 0.03 mm to 0.12 mm.

The aggregate is made of silicate and carbonate grains. The first is constituted by mono- and poly-crystalline quartz, K-feldspars, plagioclases, and micas. In all the samples, with the exception of SF1 that is characterized by a scarce presence of aggregate, grains of vulcanite, pyroxenes, plutonites and flint fragments are also present. This confirm the use of local sands in the cementitious mix-design. The sourcing area could be the surroundings of Rome that are characterised by outcrops of the so-called calcalcaline volcanic platform.

The carbonate fraction is more variable as nature and is characterized by the presence of micrites, bioclasts such as biomicrites, biosparite, biopelmicrites and intramicrites. Though the dimensions of

This project has received funding from the European Union's Horizon 2020 Research and Innovation Programme under Grant Agreement Nº 760858

the aggregate's grains vary from the sample to another, a grain-size range between 0,7 to 1,7 millimeters can be defined. In one samples (SF4) a flint fragment is up to 2.2 mm. The roundness of all the grains varies, also inside the same sample, from sub-angular to angular.

As regards the binder/aggregate ratio, the sample SF1 is practically made only of binder; the aggregate is really scarce, so that no ratio is defined. In the other samples instead the aggregate prevails on the binder in some cases with the ratio that varies from 1:2 to 1:3.

The percentage and the type of the pores are also different in all the samples, so that a hypothesis about the preparation techniques is very difficult to be made. The only consideration regards the application of the mixed mixtures. Indeed, the absence of a discontinuity between the two mortars seems to indicate a preparation of an only one mixture that was not well blended before setting up. As regard the sample SF1 it is possible the absence of aggregate addresses to hypothesise that it was a finishing layer, a sort of plaster.

It is more difficult to find in these samples a common element that permit to indicate the main characteristics of the production of this type of concrete. The use of a mixed binder, in particular the presence of air lime, evidences only the necessity of increasing the workability of the concrete and of delaying the hardening during setting.

Table 9.2. Flaminio Stadium's samples: main optical characteristics by observations on thin sections.

Sample	Binder/Aggregate ratio	Matrix	Clinker grainsize (μm)	Aggregate	Note
SF1	Only binder	Air lime + cement	50 approx.	Scarce carbonate and silicate grains	Organogenic carbonates
SF3	1:2	Air lime + cement	50 approx.	silicate and carbonate grains	silicates > carbonates. Volcanic grains
SF4	1:3	Air lime + cement	50 approx.	silicate and carbonate grains	silicates > carbonates. Volcanic grains
SF5	1:2.5	Air lime + cement	100 approx.	silicate and carbonate grains	silicates > carbonates. Volcanic grains
SF9	1:3	Air lime + cement	30 approx.	silicate and carbonate grains	carbonates ≈ silicates. Volcanic grains
SF12	1:2	Air lime + cement	120 approx.	silicate and carbonate grains	silicates > carbonates. Volcanic grains

This project has received funding from the European Union's Horizon 2020 Research and Innovation Programme under Grant Agreement Nº 760858

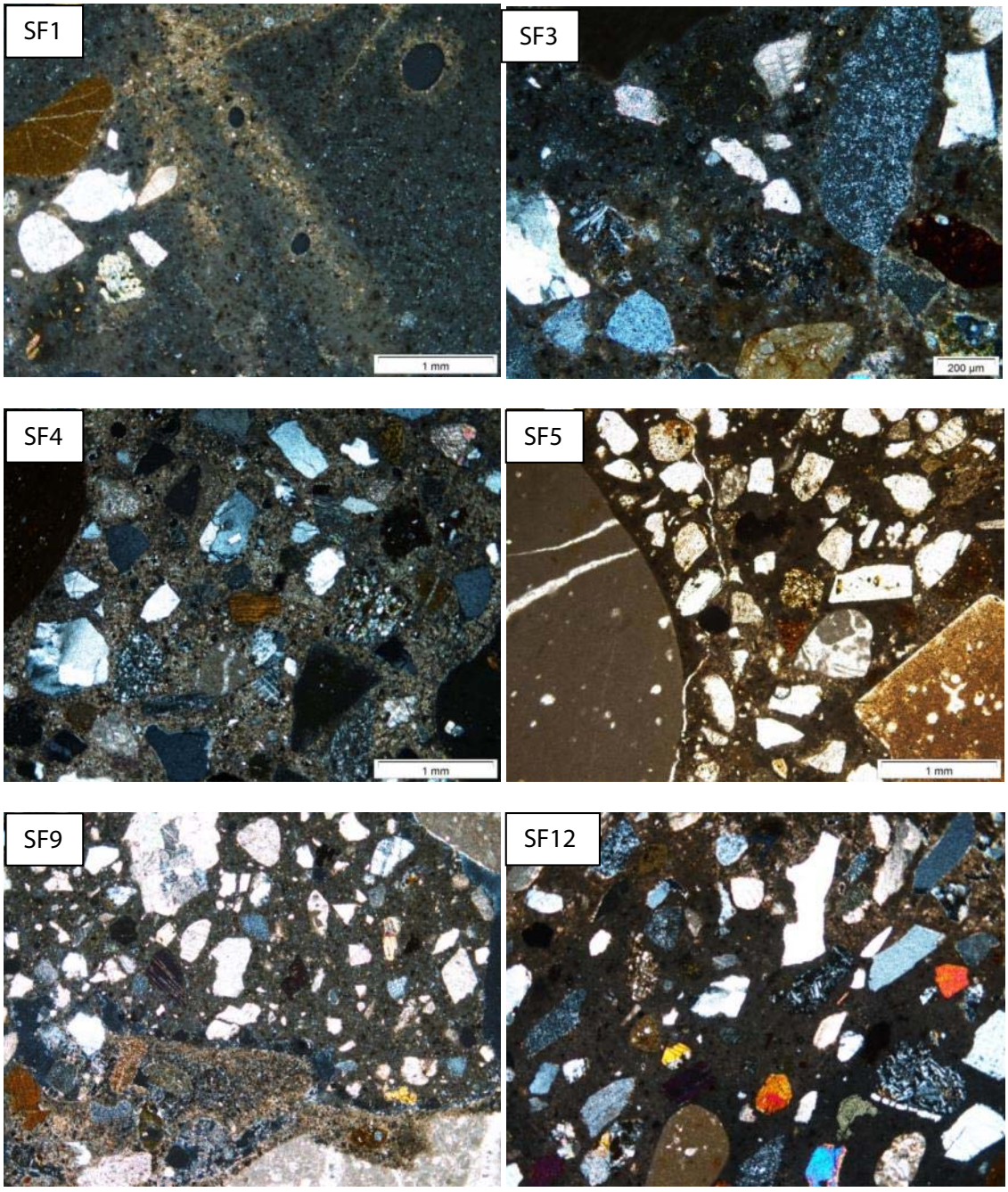

Figure 9.3. Micrographs showing the distribution of the aggregates in all the analyzed samples (XPL and PPL).

Analysis of mineralogical composition and structural properties by X-ray Diffraction, FTIR and SEM-EDS measurements

The results of XRD analyses (Table 9.3 and Fig. 9.4) show as main mineral phases quartz and calcite. A very important silicate component is present, testified by feldspars, K-feldspar, albite, pyroxenes

This project has received funding from the European Union's Horizon 2020 Research and Innovation Programme under Grant Agreement Nº 760858

and micas. Main cementitious minerals such as ettringite, alite and an anhydrous silicate calcium mineral phase are also present. In several samples, gypsum is detected and also portlandite, this last in only two samples (SF1 and SF12).

In these samples is important to note the presence of mineral phases that are compatible with the local geology.

The presence of gypsum, as said before, is connected with the necessity to hasten the grip of the mixture, while the presence of portlandite [$Ca(OH)_2$] could be explained by considering a further addition of air lime in order to probably slow down the grip.

The presence of ettringite confirmed the complete reaction and the conclusion of setting and hardening processes, while alite (C3S) and calcium silicate phases (C2S) indicate not complete reactions among the elements constituting the cementitious mixture. The contemporary presence of these mineral phases, that are the results of different firing process of the cementitious mixture, could indicates a not perfect mix design.

Table 9.3. Flaminio Stadium's samples: mineral phases composition

Sample	calcite	quartz	gypsum	feldspars	Portlandite	alite (C3S)	α-Ca_2SiO_4	Pyroxenes	Ettringite
SF1	xxx	x±	tr.	x	x±		x	x	x
SF3*	xxx	xxx	x	x			x	x	x
SF4**,*	xxx	xx		xx		x			
SF5**	xxx	xxx	x	x±		x		x	x
SF9	xxxx	x	x			x	x		x
SF11**	xxx	x±		x					x
SF12**,*	xxx	xxx		xxx	tr.				x

* traces of analcime; ** traces of micas.
Legend: xxxxx – very very abundant; xxxx – very abundant; xxx – abundant; xx – discrete; x – scarce; tr - traces

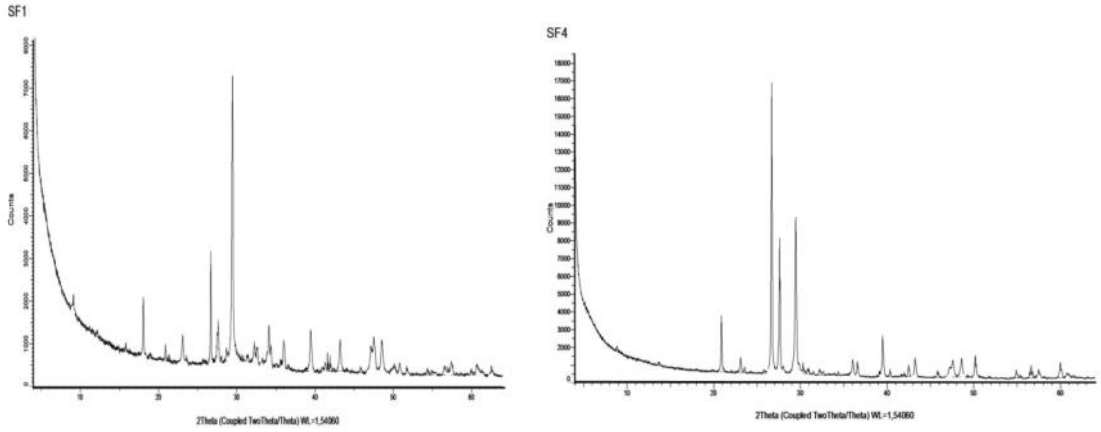

This project has received funding from the European Union's Horizon 2020 Research and Innovation Programme under Grant Agreement Nº 760858

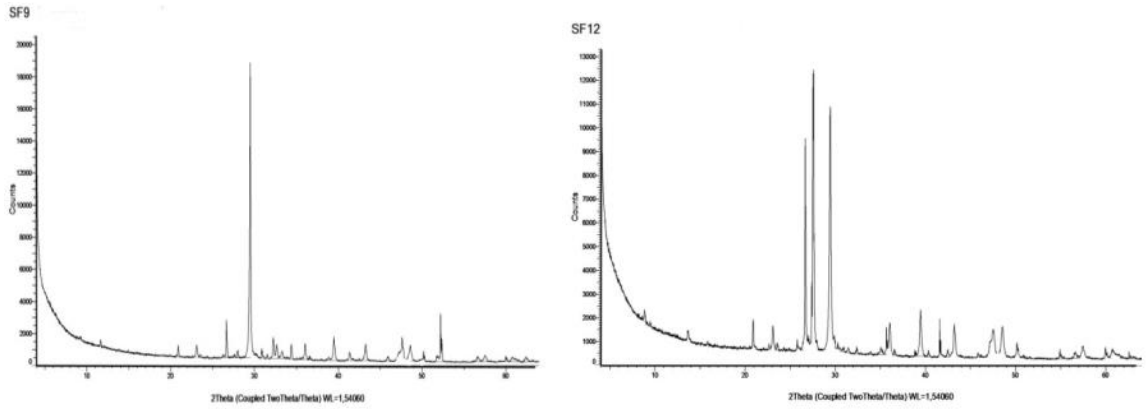

Figure 9.4. XRD spectra of some selected samples from Flaminio stadium.

The samples collected from the Flaminio Stadium were investigated also by FT-IR spectroscopy using an ATR accessory and by SEM-EDS analysis to obtain complementary information on the composition, structural and morphological properties.

The most representative data are reported hereafter by paying attention on the concrete pillars and on the undulating slabs of ferrocement.

The SEM-EDS and FTIR analyses of the samples extracted from selected external concrete pillars were carried out and the results are reported in the figures 9.5-9.6. In particular, the SF-4 and SF-5 samples from the n. 73 and n. 75 pillars, respectively, were characterized. For both the samples, it was observed among the aggregates the presence of calcite, quartz and phyllosilicates, probably micas according to XRD results. The finishing layer was also investigated and the presence of titanium oxide as main component. However, the titanium was also detected in some volcanic aggregate grains into the cementitious matrix. The SEM images clearly show differences in the shape and dimensions of the aggregate grains.

This project has received funding from the European Union's Horizon 2020 Research and Innovation Programme under Grant Agreement Nº 760858

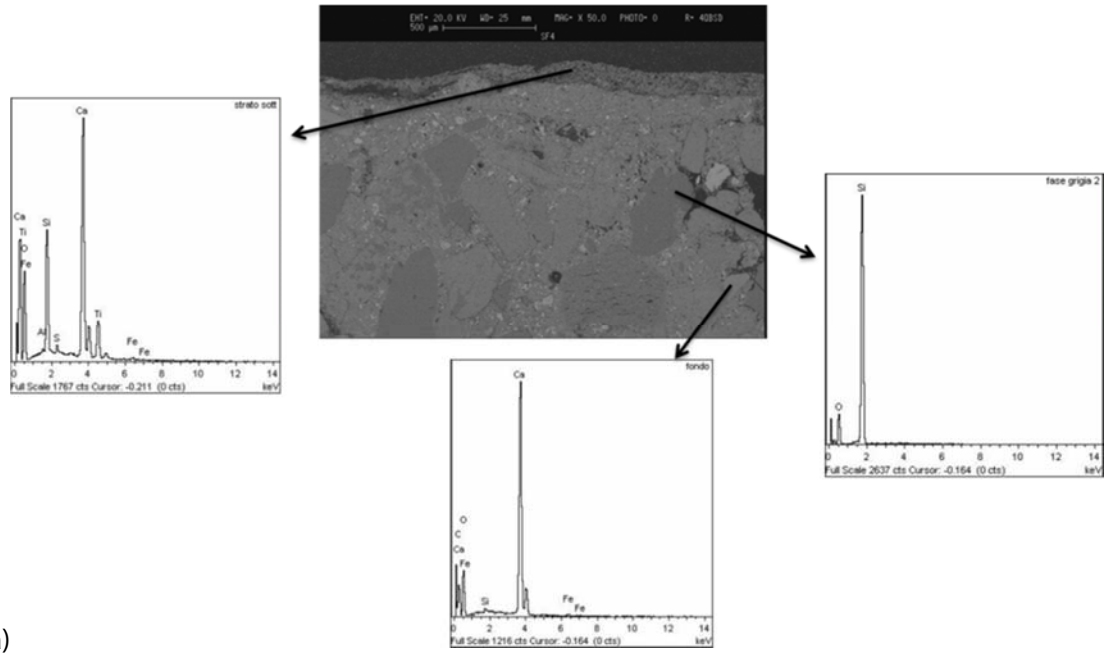

a)

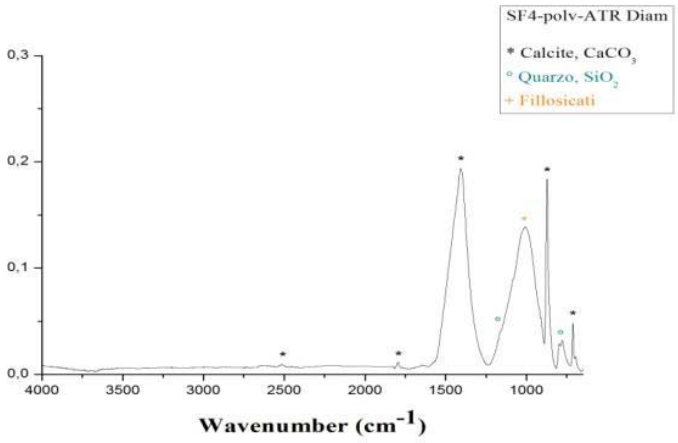

b)

Figure 9.5. a) SEM-EDS analysis and b) FTIR spectrum of SF-4 from an external concrete pillar (n. 73).

This project has received funding from the European Union's Horizon 2020 Research and Innovation Programme under Grant Agreement Nº 760858

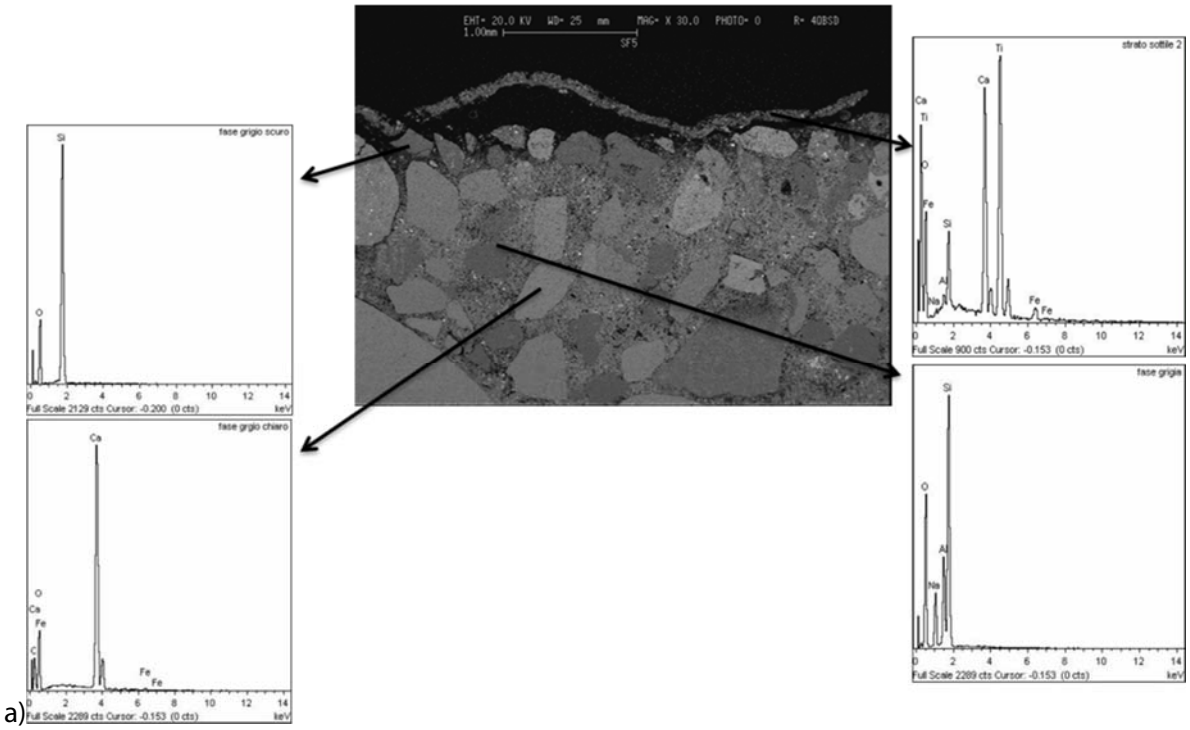

a)

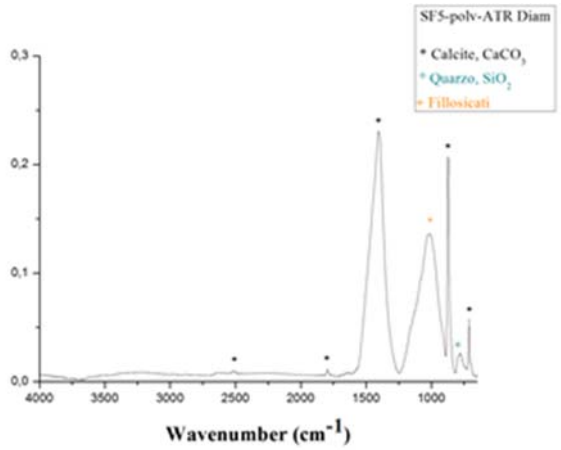

b)

Figure 9.6. a) SEM-EDS analysis and b) FTIR spectrum of SF-5 from an external concrete pillar (n. 75).

The SEM-EDS and FTIR analyses were performed also on samples extracted from selected internal concrete pillars . Some representative results are reported in the figure 9.7. In particular, the SF-9 sample from the n. 8 pillar was characterized and the results confirm mainly the presence of calcite and quartz as aggregates.

This project has received funding from the European Union's Horizon 2020 Research and Innovation Programme under Grant Agreement Nº 760858

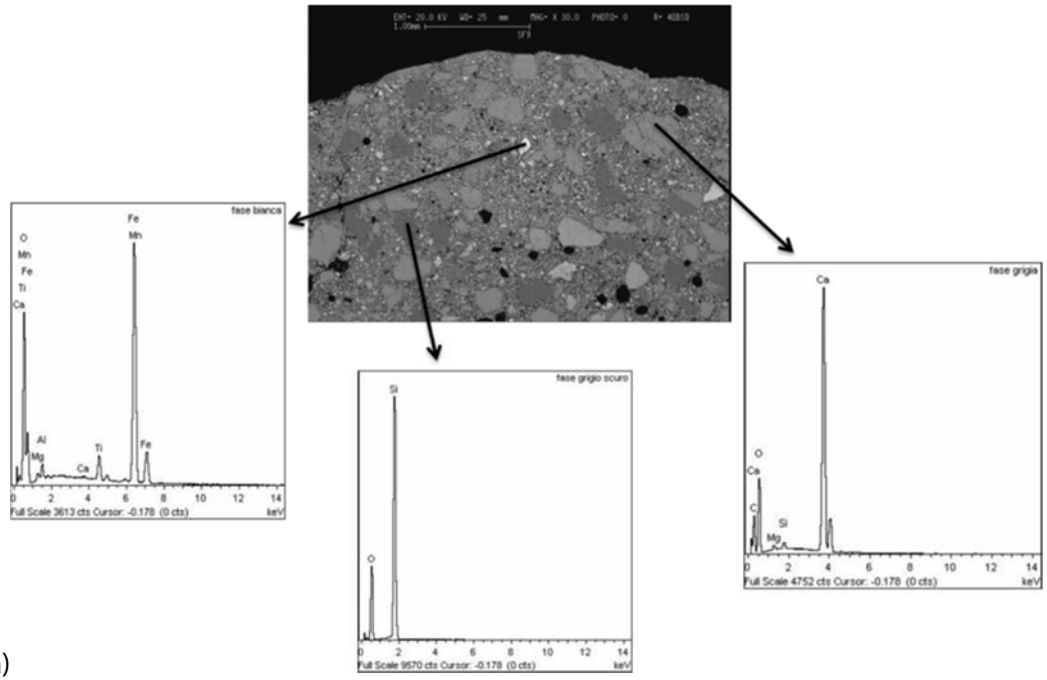

a)

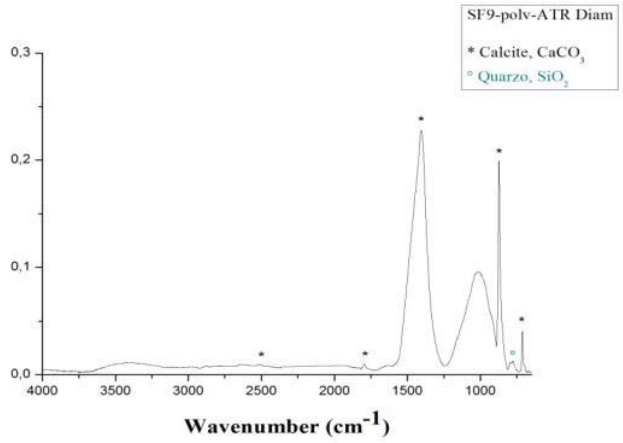

b)

Figure 9.7. a) SEM-EDS analysis and b) FTIR spectrum of SF-9 from an internal concrete pillar (n. 8).

The SEM-EDS analyses of the cross section of SF1 sample shows a cementitious matrix consisting of small aggregates. This analysis combined with FTIR measurements confirm the presence of calcite and phyllosilicates, as the main components of the aggregates (Fig. 9.8).

The radiography of this sample in figure 9.9 shows that the steel grid embedded into the ferrocement undulating slabs is still intact, without any modification due to steel degradation.

This project has received funding from the European Union's Horizon 2020 Research and Innovation Programme under Grant Agreement Nº 760858

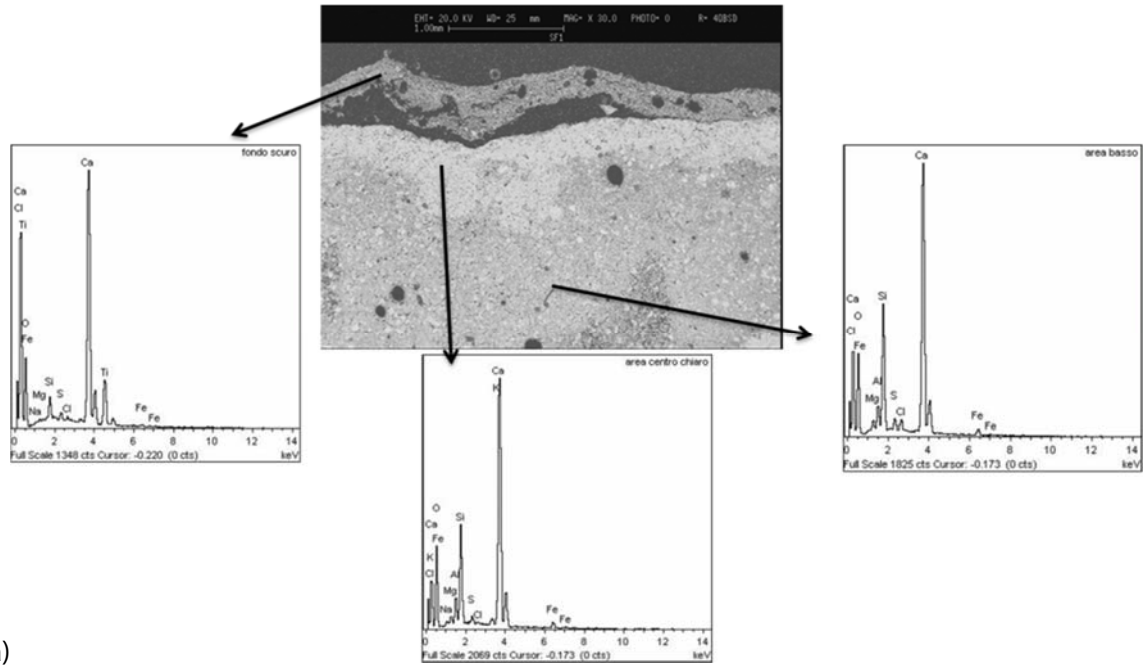

a)

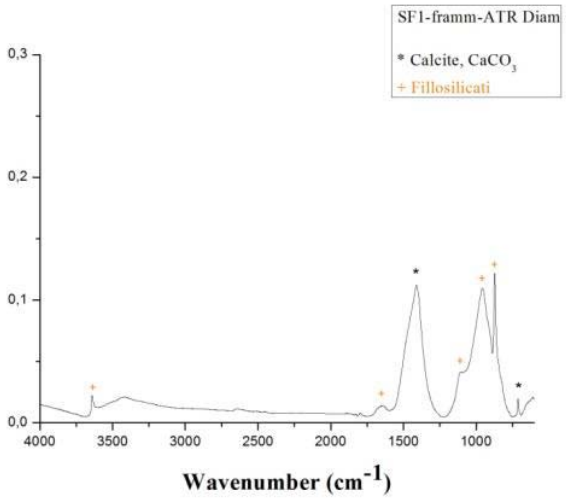

b)

Figure 9.8. a) SEM image and EDS analyses and b) FTIR spectrum of SF1 from the ferrocement canopies.

This project has received funding from the European Union's Horizon 2020 Research and Innovation Programme under Grant Agreement Nº 760858

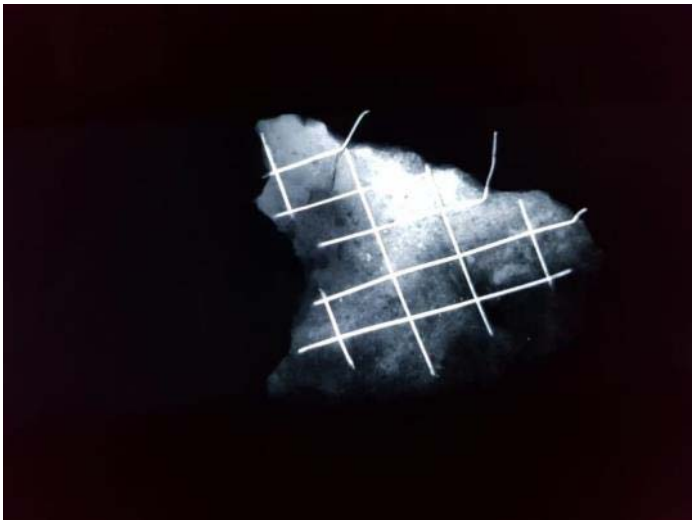

Figure 9.9. Radiography of SF-1 from the ferrocement canopies.

Porosity and pore size distribution

Only four samples out of eleven collected from the Flaminio Stadium in Rome have been analyzed by MIP technique.

The first evidence is the great heterogeneity of the samples. It is clear by observing the results of total open porosity that varies from 11% to 25% approximately (Table 9.4).

The pore size distribution (Fig. 9.10) for the samples SF3, SF5, SF12 results in a curve that covers the range 0.007-100 microns, and in which the two modes are recognizable; the first one in correspondence of small pores diameter (0.02-0.05 microns) and the other one toward diameters in the range 0.3-0.7 microns approx.

As regards the sample SF11 a Gaussian curve is defined on the base of the pore distribution covering the range 0.007-10 microns. The more frequent class, mode, is comprised between 0.03-0.07 microns.

All the curves show an asymmetric trend with a tail towards larger pores, in the range 10-100 micron.

The different behavior of sample SF11 could be probably explained by the position of the collection.

For the other samples, the presence of the two modes could be related with a possible level of degradation that resulted in the formation of larger pores at the cost of smaller ones.

Table 9.4. Flaminio Stadium samples: porosimetric results

This project has received funding from the European Union's Horizon 2020 Research and Innovation Programme under Grant Agreement Nº 760858

Sample	Open porosity (%)	Type of distribution	mode
SF3	24.68	Bimodality	
SF5	17.03	Bimodality	
SF11	11.35	Unimodality	0.03-0.07
SF512	14.23	Bimodality	

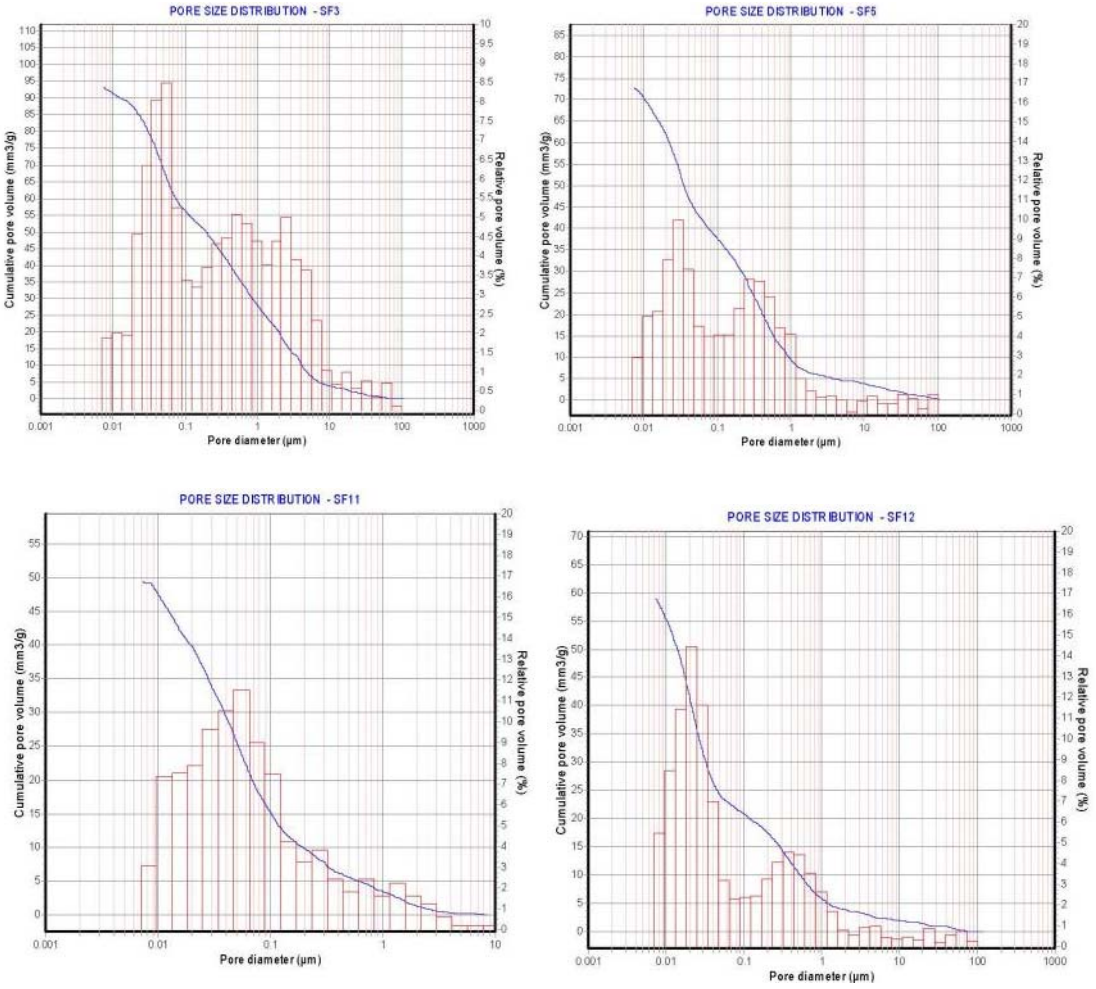

Figure 9.10. Flaminio stadium's samples: Graphs of porosimetric distributions.

Electrochemical measurements

This project has received funding from the European Union's Horizon 2020 Research and Innovation Programme under Grant Agreement Nº 760858

The electrochemical measurements (Fig. 9.11 – 9.13) were carried out to investigate the reinforcements of concrete pillars of the Flaminio Stadium and an internal concrete structure. Details on the instrument and method are reported in the previous paragraph (4.3).

Corrosion rate values related to the external concrete pillar n. 73 show that the corrosion activity is negligible for all the investigated area. Moreover, in agreement with the visual inspection, the rebars still have the surface passivation layer. It should be remembered that in this site the concrete cover is very thick (about 4 cm) and has probably protected the reinforcement from weathering.

Corrosion rate values related to the external pillar n. 9 show that also in this case the corrosion activity is negligible, similarly to the pillar n. 73. The rebars are also passivated.

From the corrosion rate map of the internal frame n. 28-29, it was observed that the left side of the wall shows a corrosion activity from moderate to high values with a peak at the bottom left corner. On the contrary, in the right side the corrosion activity is from moderate to low. Probably this difference is caused by the geometry of the prefabricated reinforced concrete that facilitates the stagnation of water at the corner elements.

This project has received funding from the European Union's Horizon 2020 Research and Innovation Programme under Grant Agreement Nº 760858

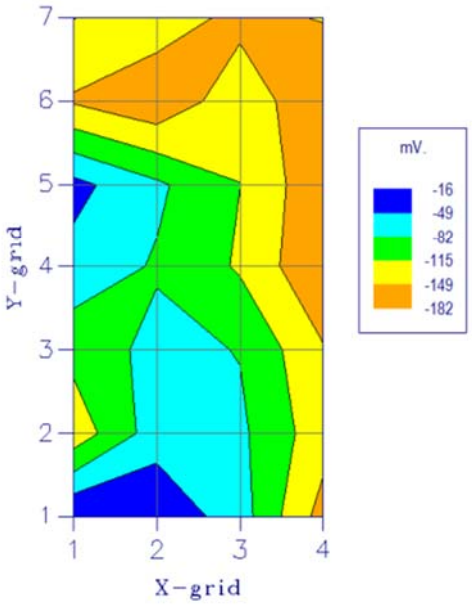

2-D surface plot of potentials - SF pillar n. 73

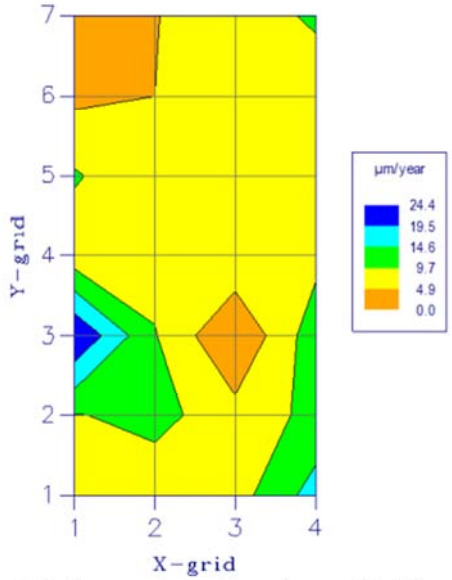

2-D surface plot of corrosion rate values - SF pillar n. 73

Y/X	1	2	3	4
7	-114 1.8 15.1	-128 4.7 14.4	-160 8.4 10.1	-147 10.1 15.9
6	-153 3.8 11.5	-178 4.9 10.5	-126 8.2 15.6	-180 8.4 9.0
5	-39 10.2 21.4	-76 6.0 18.0	-115 8.3 15.3	-177 6.4 8.8
4	-60 6.9 17.6	-85 8.2 13.1	-119 8.8 7.8	-182 8.3 6.8
3	-104 24.4 14.5	-72 9.9 20.2	-84 7.7 18.1	-146 12.5 13.3
2	-137 9.4 16.0	-64 11.4 17.6	-75 6.6 12.5	-135 11.1 5.2
1	-16 6.6 22.5	-22 6.4 19.4	-67 7.5 17.8	-163 16.7 1.8

Values in the table: Potentials mV
Corrosion rate µm/year
Resistance KOhm

Whether condition: T 12°C, RH 83 %,
Grid space used: 20cm
Steel reinforcement area: 1759 mm^2
Method of measurement: Galva Pulse

Figure 9.11. Picture of the external pillar n. 73 of the Flaminio Stadium, 2D plot of potential and corrosion rate values determined by in situ measurements, table with potential, corrosion rate and resistance values in the different X and Y positions of the surface grid.

This project has received funding from the European Union's Horizon 2020 Research and Innovation Programme under Grant Agreement N° 760858

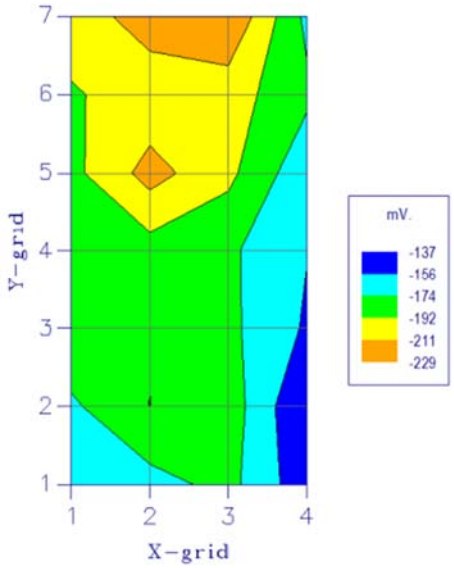

2-D surface plot of potentials - SF pillar n. 9

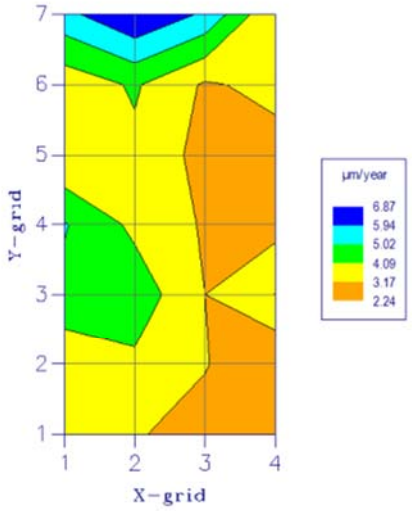

2-D surface plot of corrosion rate values - SF pillar n. 9

Y/X	1	2	3	4
7	-197 5.7 7.2	-223 6.9 7.6	-229 5.8 12.7	-169 3.2 12.7
6	-191 3.5 8.6	-196 4.2 9.8	-200 3.0 11.1	-178 3.5 12.6
5	-186 3.2 8.7	-219 3.9 11.5	-197 2.9 15.3	-161 2.8 13.4
4	-192 5.1 6.5	-184 3.9 9.5	-177 3.1 13.2	-157 2.8 13.8
3	-188 4.8 6.1	-191 4.7 6.0	-178 3.2 6.7	-154 4.1 12.5
2	-171 3.4 8.0	-192 3.9 9.2	-184 3.2 9.4	-137 2.2 9.9
1	-164 4.0 6.8	-167 3.3 8.4	-179 2.8 8.8	-144 2.4 8.6

Values in the table: Potentials mV
Corrosion rate µm/year
Resistance KOhm

Whether condition: T 10°C, RH 83 %,
Grid space used: 15cm
Steel reinforcement area: 5278 mm^2
Method of measurement: Galva Pulse

Figure 9.12. Picture of the external pillar n. 9 of the Flaminio Stadium, 2D plot of potential and corrosion rate values determined by in situ measurements, table with potential, corrosion rate and resistance values in the different X and Y positions of the surface grid.

This project has received funding from the European Union's Horizon 2020 Research and Innovation Programme under Grant Agreement Nº 760858

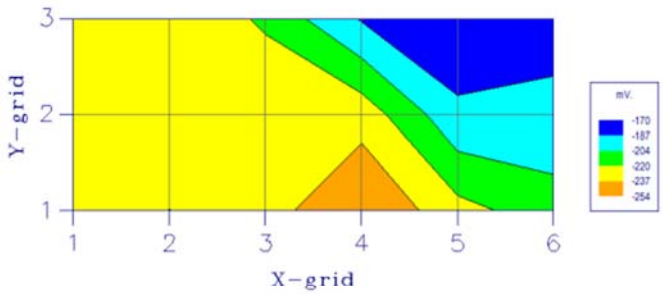

2-D surface plot of potentials - SF frame n. 28-29

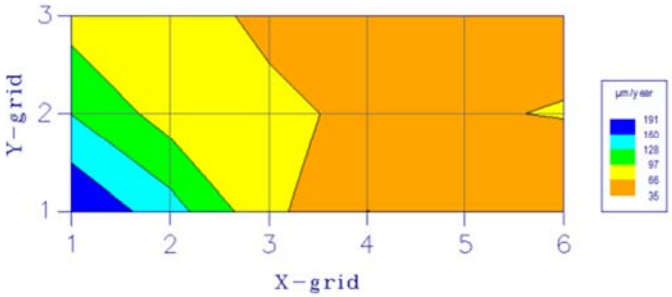

2-D surface plot of corrosion rate values - SF frame n. 28-29

Y/X	1	2	3	4	5	6
3	-222 83.8 5.2	-232 82.3 3.4	-218 57.5 5.0	-186 41.7 9.5	-170 49.6 10.6	-179 56.1 5.9
2	-226 127 2.5	-236 82.6 2.3	-233 75.5 2.7	-230 57.4 5.4	-191 63.6 8.7	-192 67.6 7.6
1	-228 191 2.3	-220 141 2.6	-254 34.7 13.3	-254 34.7 13.3	-226 49.8 12.0	-211 35.8 8.8

Values in the table: Potentials mV
Corrosion rate µm/year
Resistance KOhm

Whether condition: T 18°C, RH 81 %, rain
Grid space used: 20cm
Steel reinforcement area: 1759 mm^2
Method of measurement: Galva Pulse

Figure 9.13. Picture of the internal concrete frame n. 28-29 of the Flaminio Stadium, 2D plot of potential and corrosion rate values determined by in situ measurements, table with potential, corrosion rate and resistance values in the different X and Y positions of the surface grid.

Schmidt Hammer Test

The rebound number (R) measured in different zones of the Flaminio Stadium has been correlated with the correspondent value of hardness as indicated in the conversion curves for the rebound instrument type L, on the basis of the horizontal impact.

Taking into consideration the average classes of resistance (From Table 3.1 of the Eurocode 2, EN 1992-1-1), the concrete present in the monumental test site has a very good resistance (≥ 60/70) in the two pillars examined placed in the external part of the structure (side Viale Tiziano) made of sound reinforced material. In the case of the internal pillar (number 37 at first level) the concrete shown a little bit lower resistance.

This project has received funding from the European Union's Horizon 2020 Research and Innovation Programme under Grant Agreement N° 760858

Table: Classes of resistance of concretes

CLASS OF RESISTANCE	fck (Mpa)	Rck (Mpa)	CONCRETE CLASS EN 206
C 16/20	16	20	low
C 20/25	20	25	
C 25/30	25	30	medium
C 32/40	32	40	
C 40/50	40	50	
C 45/55	45	55	
C 50/60	50	60	high
C 55/67	55	67	
C 65/70	65	70	
C 70/85	70	85	
C 80/95	80	95	very high
C 90/105	90	105	
C 100/115	100	115	

Correlation curve for rebound type L

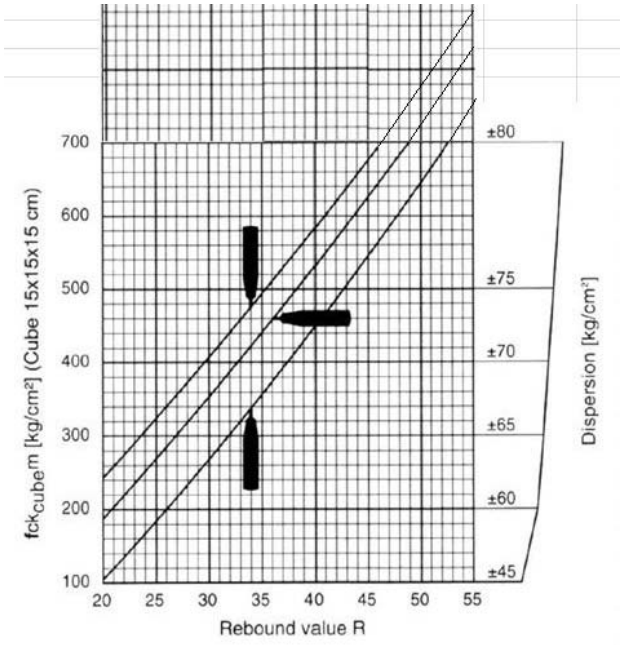

This project has received funding from the European Union's Horizon 2020 Research and Innovation Programme under Grant Agreement Nº 760858

Pilllar 73 Entrance 36 PQ 1°floor Rebound type L

Pilllar 73 Entrance 36 PQ 1°floor

Cm from ground	number	sx	dx
170	3_4	48	49.5
152	5_6	42	42
124	7_8	41	40
	mean	43.8	
	st dev	4.0	
	Kg/cm2	605	± 75
	MPa	**59.3**	± 7.3
104	9_10	34	50
95	11	39	
86	12_13	**50**	42
	mean	43.0	
	st dev	7.0	
	Kg/cm2	590	± 75
	MPa	**57.8**	± 7.3
67	14_15	44	44
47	16_17	43	46
37	18	40	
	mean	43.4	
	st dev	2.2	
	Kg/cm2	595	± 75
	MPa	**58.3**	± 7.3

	Rvalue	
mean	43.41	
st dev	4.44	
Kg/cm2	590	± 75
MPa	**57.8**	± 7.3

This project has received funding from the European Union's Horizon 2020 Research and Innovation Programme under Grant Agreement Nº 760858

Pillar 8 external

Cm from ground	number	sx	cent	dx
132	1_2_3	50	52	52
110	4_5_6	49.5	50.5	51
	mean		51.1	
	st dev		0.89	
	Kg/cm2		750	± 80
	MPa		**73.5**	± 7.8
92	7_8_9	50	51	48
70	10_11_12	52	50	48
	mean		49.8	
	st dev		1.60	
	Kg/cm2		720	± 80
	MPa		**70.6**	± 7.8
42	S1_2_3	50	47	48
24	S4_5_6	46	48	48
	mean		47.8	
	st dev		1.33	
	Kg/cm2		680	± 80
	MPa		**66.6**	± 7.8

	R	
mean	49.5	
st dev	1.85	
Kg/cm2	720	± 80
MPa	**70.6**	± 7.8

This project has received funding from the European Union's Horizon 2020 Research and Innovation Programme under Grant Agreement Nº 760858

Pilllar 9 external

Cm from ground	number	sx	cent	dx
132	1_2_3	54	46	51
110	4_5_6	47	48	50
	mean		49.3	
	st dev		2.94	
	Kg/cm2		705	± 80
	MPa		**69.1**	± 7.8
85	7_8_9	44	50	45
66	10_11_12	51	44	48
	mean		47.0	
	st dev		3.10	
	Kg/cm2		660	± 75
	MPa		**64.7**	± 7.3
30	13_14_15	50	50	50
16	16_17_18	51	42	50
	mean		48.8	
	st dev		3.37	
	Kg/cm2		700	± 80
	MPa		**68.6**	± 7.8

	R	
mean	48.4	
st dev	3.13	
Kg/cm2	690	± 75
MPa	**67.6**	± 7.3

Correlation data between R values and Compressive strength (MPa)

SF Zone	R value	Kg/cm^2	MPa
Pillar 37	43.41	555	**54.4**
Pillar 8	49.5	720	**70.6**
Pillar side right 8	48.4	690	**67.7**

Measurement of moisture content and salts content

The SUSI measurements have been done in some of the selected zones (pillar 73, pillar 8 and pillar 9) and in the same points selected for the Schmidt Hammer tests. Taking into account the results of rebound test, the low value of the salinity index (SI, that determines presence of electrolytes), confirms the good quality of the pillars. In all the inspected pillars the presence of rising dampness were detected. No relevant rate of presence of salts was detected on all investigated zones, this can be interpreted as a low risk of decay factor for the cement integrity.

This project has received funding from the European Union's Horizon 2020 Research and Innovation Programme under Grant Agreement Nº 760858

Pilllar 73 Entrance 36 PQ 1 floor

Distance from ground [cm]	number	Moisture content			
		sx	cent	dx	average
190	11P	0.8	1.6	1.2	***1.2***
171	10P	2.0	2.4	2.2	***2.2***
152	9P	2.0	1.4	1.4	***1.6***
133	8P	1.6	1.6	1.0	***1.4***
123	7P	1.6	1.2	2.2	***1.7***
104	6P	1.0	1.4	0.4	***0.9***
86	5P	1.4	1.0	1.4	***1.2***
66	4P	1.4	0.6	1.6	***1.2***
46	3P	2.4	2.0	1.6	***2.0***
36	2P	2.8	2.2	2.0	***2.3***
17	1P	3.0	1.4	2.4	***2.3***

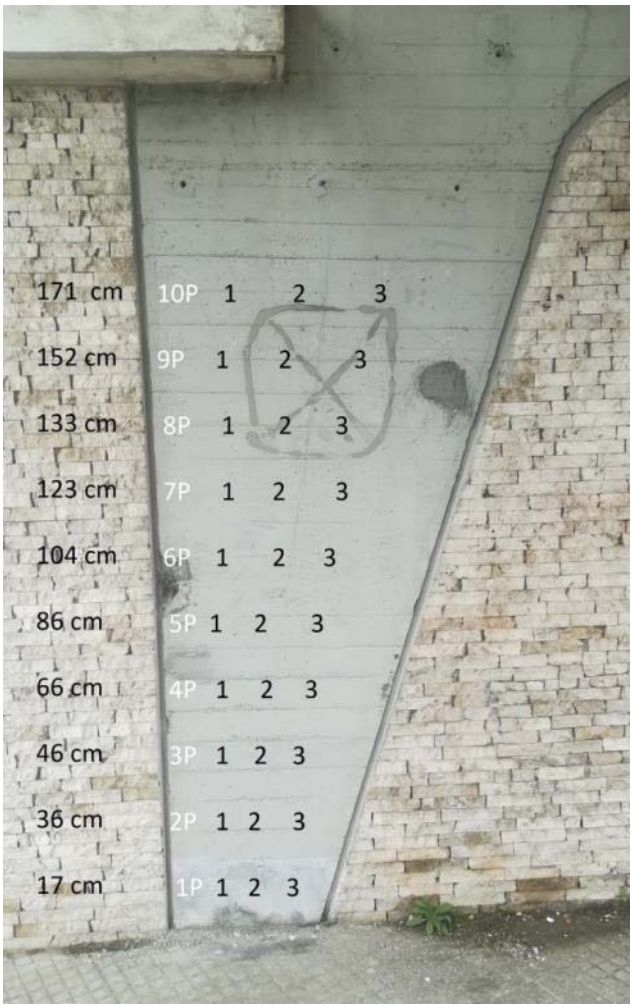

This project has received funding from the European Union's Horizon 2020 Research and Innovation Programme under Grant Agreement Nº 760858

Pillar 8 external

Distance from ground [cm]	number	Moisture content			
		sx	cent	dx	media
132	6S	2.2	2.2	2.0	***2.1***
110	5S	0.8	2.2	1.6	***1.5***
92	4S	1.6	2.2	1.6	***1.8***
70	3S	2.2	1.6	2.2	***2.0***
42	2S	1.6	1.4	1.4	***1.4***
24	1S	2.0	2.2	2.8	***2.3***

Pilllar 9 external

Distance from ground [cm]	number	Moisture content			
		sx	cent	dx	media
132	6D	2.6	3.2	2.4	***2.7***
110	5D	1.8	3.2	2.2	***2.4***
85	4D	1.6	2.6	2.2	***2.1***
66	3D	3.2	2.2	1.8	***2.4***
30	2D	2.6	2.2	2.2	***2.3***
16	1D	1.8	2.1	2.0	***2.0***

This project has received funding from the European Union's Horizon 2020 Research and Innovation Programme under Grant Agreement N° 760858

Bonded water and carbonation of cement paste in the concrete (DTA/TG)

All the samples from Flaminio stadium show the typical thermal curves of hydraulic materials (figure 9.14) that means a continuous weight loss in the investigated temperature range, and in particular in the range 110-750°C that is 10% on average. The results of the investigation are reported in the table 9.5, in which the percentage in weight losses were calculated when possible, while in other cases the possible presence of the mineral phases linked to correspondent the weight loss has been only indicated. The obtained results are in accordance with those of XRD investigation.

Table 9.5. Flaminio stadium's samples: results of thermal investigations.

Sample	110-750°C	750°C (calcite)	Ettringite	Gypsum	Portlandite
SF 1	13 %	20 %	x	tr.	1.5 %
SF 3	8 %	30 %		3 %	
SF 4	7 %	22 %		tr	
SF 5	10 %	20 %			
SF 9	7 %	32 %		tr	
SF 11	8 %	43 %	x		
SF 12	15 %	20 %	x		

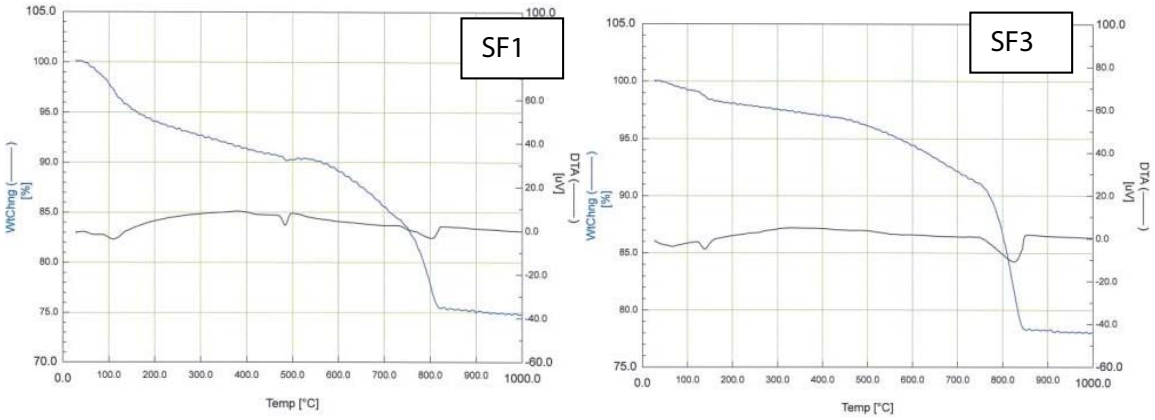

This project has received funding from the European Union's Horizon 2020 Research and Innovation Programme under Grant Agreement Nº 760858

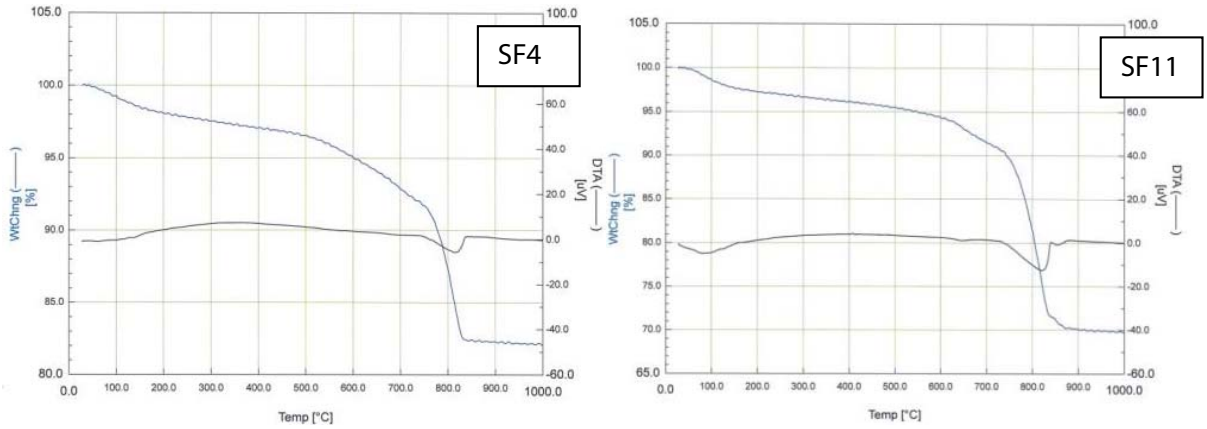

Figure 9.14. Flaminio Stadium's samples: thermal spectra.

1.3.1 Compositional and textural properties of concrete

The characterization of the samples from the Flaminio Stadium showed the use of mixed mortar obtained by mixing air lime and clinker. The so not well merged mixture it is indicative of an approximate approach to the preparation of the mortar. It is more probable that the lime was used to favor the make easy and to slow the setting up and the hardening of the concrete. In only one sample traces of portlandite [Ca(OH)2] are present. Different hypotheses can be made to explain it: not complete carbonation of the concrete components; recent restoration intervention; rehydration phenomena of carbonate phases due to prolonged contact with water.

It is possible to point out the use of local materials in terms of aggregates. The volcanic aggregates in the Flaminio Stadium can derive from outcrops of Campania-Latium volcanism.

1.3.2 State of conservation of the monument

The Flaminio Stadium is now in a serious state of degradation since it was abandoned for years (Fig. 9.15). The decay processes are mainly due to improper interventions that failed to respect the characteristics of the original structure, widespread deterioration caused by years of neglect and the physiological aging of the materials.

The damages are mainly due to water infiltration into concrete structure and to the notable formation of biodeteriogens such as algae and fungi. Salt efflorescence is visible in some parts of the structure and contributes to the deterioration of concrete. However, the results of the characterizations confirm that the concrete pillars are still in a good state of conservation with a

This project has received funding from the European Union's Horizon 2020 Research and Innovation Programme under Grant Agreement Nº 760858

medium-high consistency of concrete and steel reinforcements. The pictures below show the major degradation problems that were observed in some areas of the stadium, mainly due to the lack of appropriate maintenance actions and to a not optimal drainage of water probably caused by the improper interventions.

Figure 9.15. Panoramic view and details of the state of conservation of the Flaminio Stadium.

This project has received funding from the European Union's Horizon 2020 Research and Innovation Programme under Grant Agreement Nº 760858

1.3.3 Mapping of the damages

The pictures in figure 9.16 show the most advanced types of degradation in the different areas of the monument.

Red: water infiltration, formation of biodeteriogens, detachments and iron corrosion;

Blue: corrosion of metal reinforcement;

Yellow: salt efflorescence;

Green: detachments of concrete material;

Violet: damp areas.

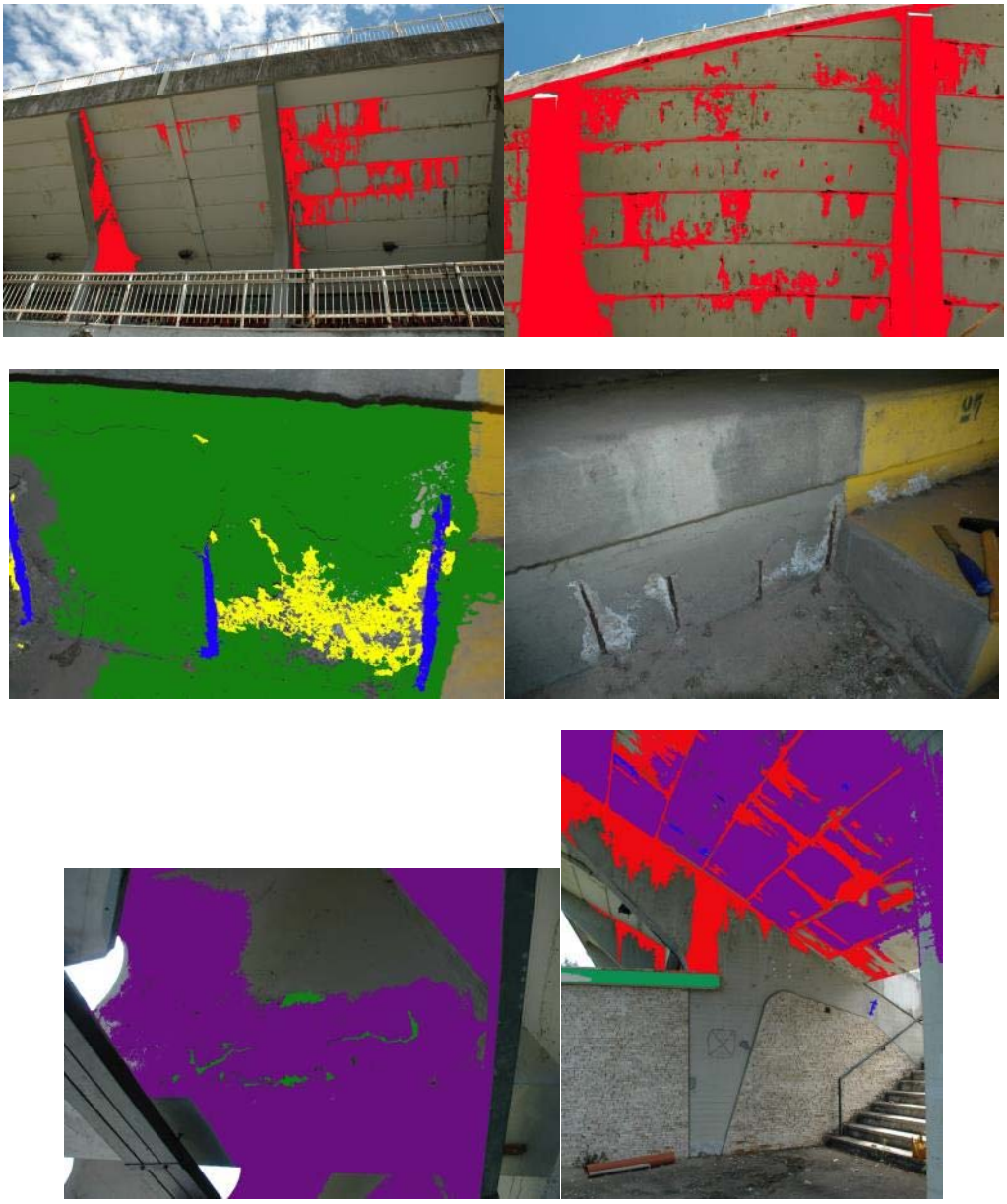

This project has received funding from the European Union's Horizon 2020 Research and Innovation Programme under Grant Agreement Nº 760858

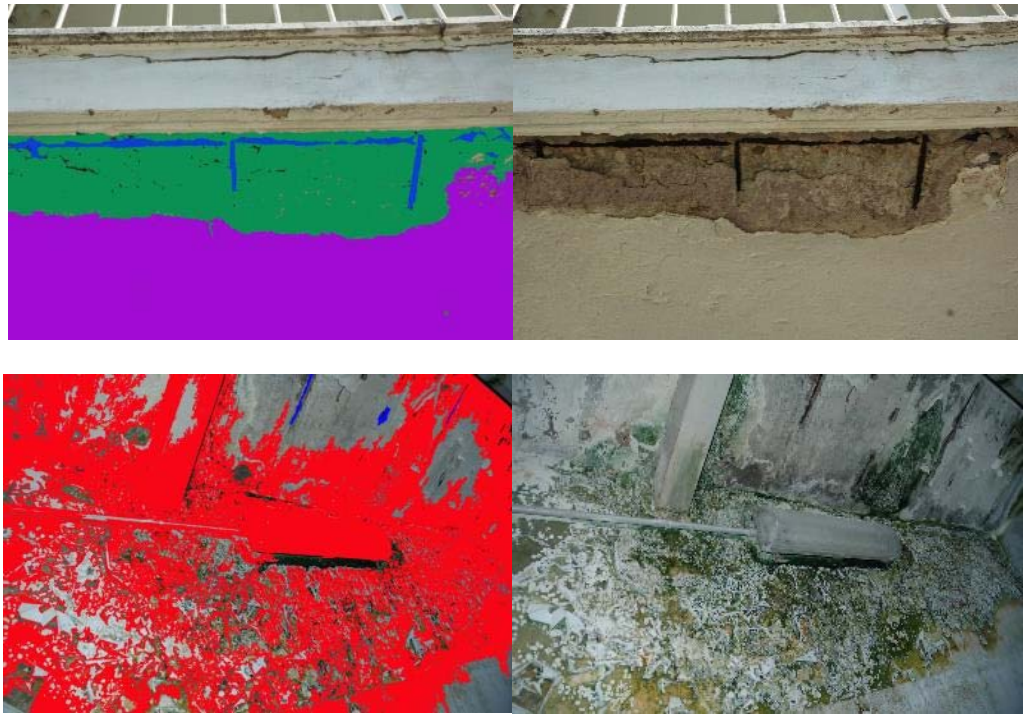

Figure 9.16. Damage maps in panoramic view and in details of the Flaminio Stadium.

1.4 Summary

The characterization activities have make possible to learn more about the manufacturing characteristics of the Flaminio Stadium and also about the innovative ideas and ways to use concrete proposed by Pier Luigi Nervi. Moreover, it was possible to obtain further information about the conservation problems, identifying the main causes of deterioration and the well-preserved areas. The conservation problems are caused mainly by the infiltration of water in some areas of the concrete structure. On the contrary, other elements are still in a good state of conservation.

As result of the characterization, the high heterogeneity in terms of dimensions and shape of aggregates and residues of clinker puts in evidence raw materials and working processes different during the building of the stadium. In addition, the concrete samples constituting the Flaminio Stadium are made of mortars with two different components as binder: air lime and clinker. It is possible that the presence of air fraction was used to obtain a product more workable and with long time of hardening. At the same time, this component decreases the mechanical properties. These two components are not well blended, influencing the durability of the mortars and the values of the compressive strengths as measured by using the Schmidt Hammer test.

This project has received funding from the European Union's Horizon 2020 Research and Innovation Programme under Grant Agreement Nº 760858

The definition of an appropriate conservation plan is mandatory to preserve this concrete monument. The Flaminio Stadium has been now listed, thus recognizing its unique value. The application of the InnovaConcrete products based on consolidants and corrosion inhibitors can play a key role in the preservation of this monument and in the inhibition of degradation processes. The application of products with superhydrophobic properties can also have a relevant role in the inhibition of degradation processes due to water infiltration and in the conservation of this monument.

This project has received funding from the European Union's Horizon 2020 Research and Innovation Programme under Grant Agreement Nº 760858